

## Supporting Information:

### ***Low Loss Optical Waveguiding in Large Single Crystals of a Thiophene-Based Oligomer***

Sajedeh Motamen<sup>1</sup>, Christian Schörner<sup>2</sup>, Dominic Raithe<sup>2</sup>, Jean-Pierre Malval<sup>3</sup>, Thibaut Jarrosson<sup>4</sup>, Françoise Serein-Spirau<sup>4</sup>, Laurent Simon<sup>3</sup>, Richard Hildner<sup>2</sup>, Günter Reiter<sup>1</sup>

<sup>1</sup>Physikalisches Institut, Albert-Ludwigs-Universität, 79104 Freiburg, Germany

<sup>2</sup>Experimentalphysik IV, University of Bayreuth, 95440 Bayreuth, Germany

<sup>3</sup>Institut de Sciences des Matériaux de Mulhouse IS2M, LRC 7228-CNRS-UHA, 4 rue des Frères Lumière, 68093 Mulhouse, France

<sup>4</sup>Institut Charles Gerhardt de Montpellier, UMR 5353-CNRS Equipe Architectures Moléculaires et Matériaux Nanostructurés (AM2N), Ecole Nationale Supérieure de Chimie de Montpellier, 8 Rue de l'Ecole Normale, 34296 Montpellier cedex 05, France

The room-temperature PL spectrum from the body of a 3TBT single crystal is displayed in Figure S1. We attempted to represent the data by the smallest possible number of Gaussian functions. Yet, to accurately reproduce the spectrum, we had to fit five Gaussian peaks, as detailed recently.<sup>1</sup> The full width at half maximum (FWHM) and the intensity of the Gaussians were treated as adjustable parameters to give the best fit to the experimental data. Out-coupled PL spectrum at the tip of crystal was decomposed into four Gaussian peaks because the intensity of the highest energy peak was reduced so strongly that it was not possible to decompose the spectra into the five peaks. The decomposition procedure is illustrated in Figure S2. It should be mentioned that all of the fitting parameters, except the relative intensities, did not vary significantly for all spectra measured at different propagation distances (table S1 and S2).

To justify the use of four to five Gaussian functions to fit the room temperature PL, we also have taken low temperature PL spectra at 1.5 K from a single crystal (Figure S3). The PL from the body exhibited three dominating peaks, yet, these spectra had to be decomposed into eight Gaussian peaks, which correspond to different vibronic modes (Figure S3). Peak A can

be ascribed to the purely electronic 0-0 transition of 3TBT molecule. In most thiophene-based molecules, the symmetric stretching vibronic mode (e.g., aromatic carbon-bond stretch, energy  $\approx 170$  meV or  $1400\text{ cm}^{-1}$ ) couples strongly to the electronic transition. Thus, we consider the peaks E and H (with a spacing of approximately 170 meV) as the 0-1 and 0-2 vibronic peaks of this stretching mode, respectively. Peak B is attributed to vibrational modes either of the thiophene backbone or to a liberation motion of the rings within the backbone. Peaks C and D are attributed to ring breathing modes of thiophene and benzene. Peak G is probably a combination of vibrations, e.g from peak D (ring breathing) and peak E (carbon bond stretch). For details, see ref<sup>1</sup>.

As the line widths (FWHM) of the peaks increased with temperature, neighboring lines separated by less than ca. 60 meV could not be resolved in the room temperature spectra. Consequently, some peaks of the PL spectra measured at room temperature contained a superposition of two low temperature peaks. Peak 1 of the room temperature data can be assigned to a superposition of the low temperature peaks A and B. Peak 2 is probably a superposition of peaks C and D and peak 4 a superposition of peaks F and G.

The low temperature PL spectrum measured at the tip of the crystal (Figure S3a, thick blue line; the distance between tip and the location of excitation was  $20\mu\text{m}$ ) featured significant differences compared to the body spectrum especially in the high-energy region. Comparing these spectra indicated that the 0-0 peak seemed to disappear nearly entirely already after short guided distance (FigureS3a). Figure S3b (hatched bars) shows the observed relative changes in intensity of the various Gaussian peaks of the PL spectra recorded at the tip and body of the crystal, respectively, using seven and eight Gaussian peaks for decomposition. Importantly, only the intensities of the Gaussians changed, their center energies and line widths stayed almost constant.

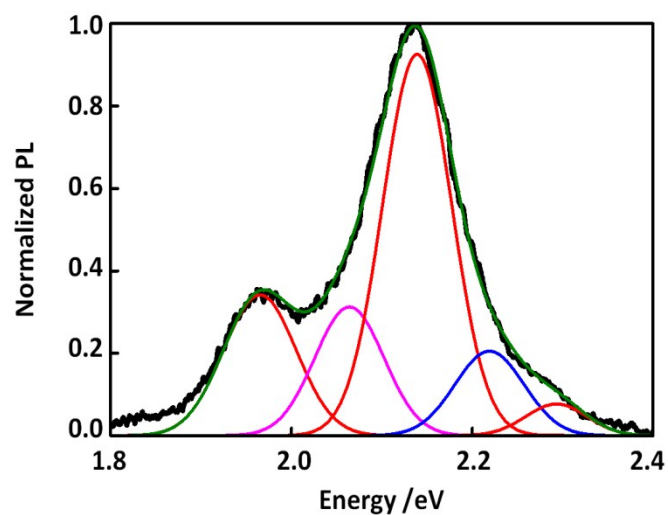


Figure S1: Normalized PL spectrum (black curve) from the body of a 3TBT **crystal** at room temperature, together with a fit (green curve) of five Gaussian peaks to reproduce the vibronic structure. The diameter of the detection area was 1  $\mu\text{m}$  and the width of crystal was 4  $\mu\text{m}$ .

| Gaussian | Peak position [eV] | Integrated Area | Full Width at Half Maximum FWHM [eV] | Intensity at Peak Position [Counts] | Relative Integrated Area [%] |
|----------|--------------------|-----------------|--------------------------------------|-------------------------------------|------------------------------|
| Peak 1   | 2.293              | 0.004           | 0.08                                 | 0.05                                | 2.70                         |
| Peak 2   | 2.22               | 0.019           | 0.09                                 | 0.20                                | 10.97                        |
| Peak 3   | 2.14               | 0.087           | 0.09                                 | 0.90                                | 50.33                        |
| Peak 4   | 2.064              | 0.029           | 0.09                                 | 0.30                                | 17.03                        |
| Peak 5   | 1.965              | 0.033           | 0.095                                | 0.32                                | 18.95                        |

TableS1. Fitting parameters used for the decomposition of photoluminescence spectra from the body of the **crystal** in Figure S1.

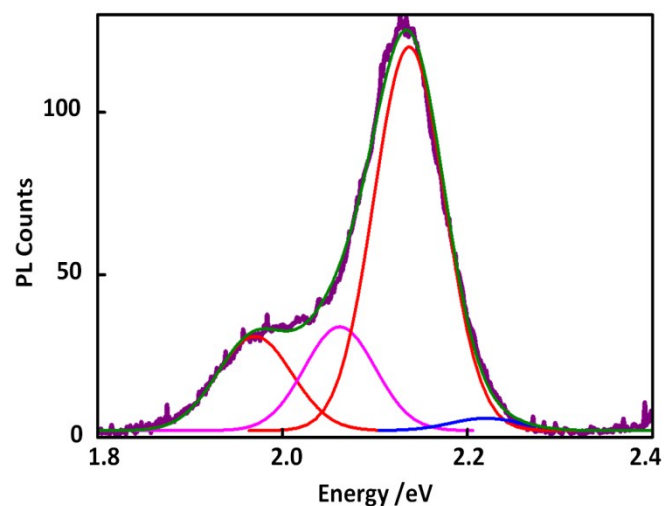


Figure S2: PL spectrum of the out-coupled light from a single crystal after a propagation distance of 7  $\mu\text{m}$  at room temperature (violet curve) together with a fit (green curve) of four Gaussian peaks to reproduce the vibronic structure. The PL spectrum was weighted according to the procedure described in the main text. The diameter of the excitation area at body and detection area at tip was 64  $\mu\text{m}$  and 8  $\mu\text{m}$ , respectively.

| Gaussian | Peak Position [eV] | Integrated Area | Full Width at Half Maximum FWHM [eV] | Intensity at Peak Position [Counts] | Relative Integrated Area [%] |
|----------|--------------------|-----------------|--------------------------------------|-------------------------------------|------------------------------|
| Peak2    | 2.22               | 0.36            | 0.09                                 | 3.80                                | 2.06                         |
| Peak3    | 2.137              | 11.31           | 0.09                                 | 118.12                              | 64.02                        |
| Peak4    | 2.062              | 3.06            | 0.09                                 | 31.94                               | 17.31                        |
| Peak5    | 1.97               | 2.93            | 0.095                                | 29.01                               | 16.59                        |

TableS2. Fitting parameters used for out-coupled light at the tip of a single crystal (Figure S2) after a propagation distance of 7  $\mu\text{m}$  at room temperature.

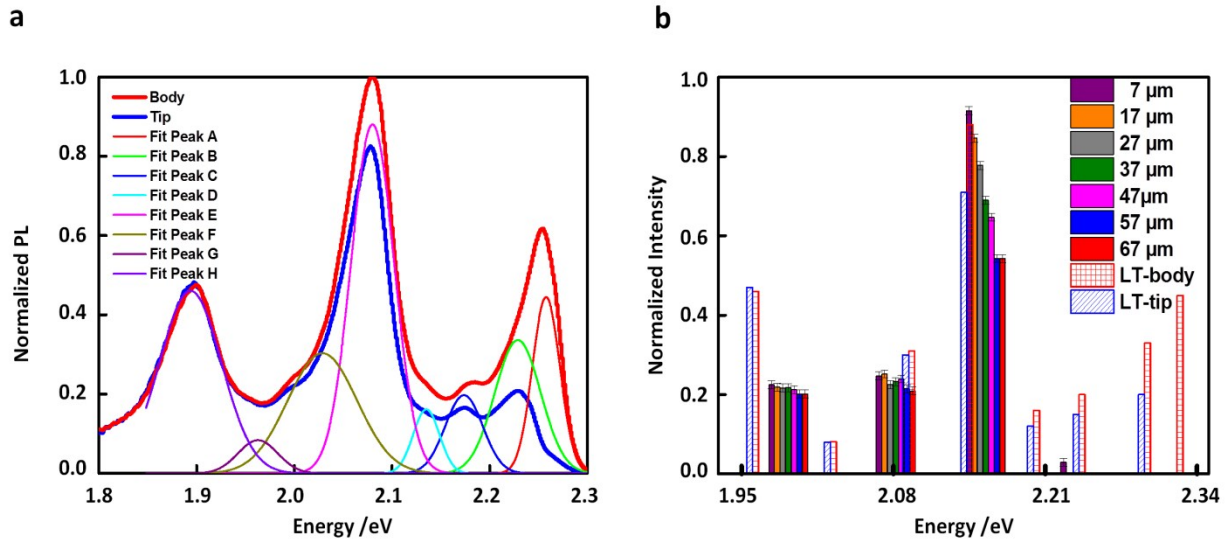
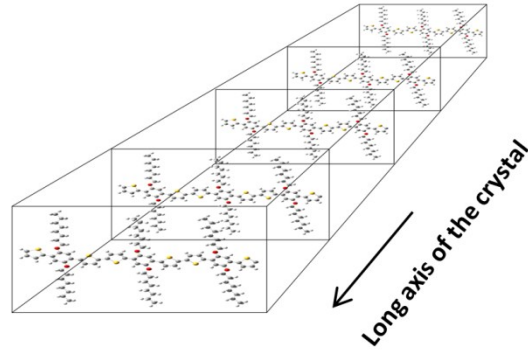


Figure S3. a) Normalized PL spectra of excitation region (body, thick red curve) and out-coupled waveguided part (tip of the crystal, after 20  $\mu\text{m}$  waveguiding) (thick blue curve) at 1.5 K. Both spectra were fit with a series of Gaussian functions exemplified here for the body spectrum, b) Hatched bars: Intensity of the Gaussian peaks fitted to the PL spectra of a tip and body of the 3TBT single crystal at 1.5 K. Filled bars: Intensities of the Gaussian functions fitted to the room temperature PL spectra from the tip of a crystal as function of the distance between excitation and tip (For a better comparison, emission peaks measured at 1.5 K were shifted manually by +0.070 eV, the width of the bars was chosen to be 0.008 eV). The position of a given emission peak at room temperature was always the same independent of the distances to the excitation area (as a reference, we took the emission at a distance 7  $\mu\text{m}$  from the excitation area). However, for better visibility, we shifted the positions manually by 0.01 eV with respect to the peak on the left. (Width of the bars was chosen to be 0.008 eV).

a



b

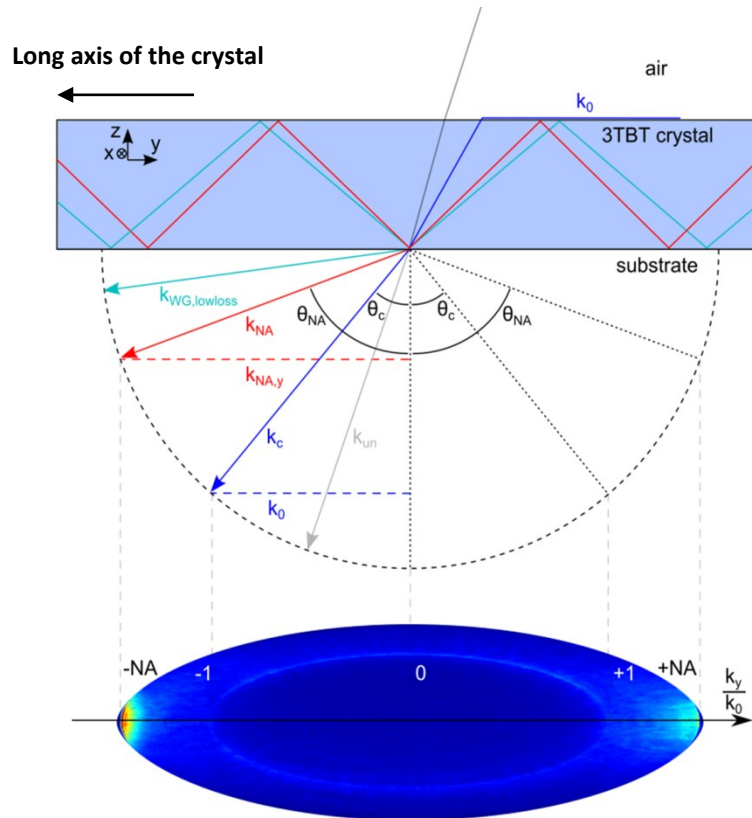


Figure S4: a) Schematic illustration of 3TBT molecule within the crystal. b) Schematic illustration of the principle of back focal plane (BFP) imaging for our sample geometry of a 3TBT crystal placed on a glass substrate in air. The substrate is index-matched to the objective using immersion oil. The photoluminescence of the 3TBT crystal is distributed in the objective's back focal plane according to its in-plane wavevector components ( $k_i$ , with  $i = x, y$ ) in the substrate, which are normalized to the magnitude of the wavevector in air ( $k_0$ ). The BFP image (bottom) exhibits two characteristic circles with radii of  $|k_i|/k_0 = 1$  and  $|k_i|/k_0 = NA$ . These rings can be translated into two characteristic angles  $\theta_c$  and  $\theta_{NA}$  for the direction of the detected PL into the substrate using geometric considerations (top): For the inner ring with angle  $\theta_c$  the condition for total internal reflection at the crystal - air interface is exactly fulfilled, see blue line labelled with the wavevector  $k_c$ . The in-plane magnitude of  $k_c$  is thus exactly  $k_0$ . The outer ring translates into the maximum collection angle  $\theta_{NA}$  given by the numerical aperture (NA) of the objective (cf. red wavevector  $k_{NA}$ ). The corresponding maximum in-plane wavevector component is accordingly  $k_{NA,i} = k_0 \cdot NA$ . Emission propagating at still higher angles is not collected by our setup, yet such emission experiences very low loss during waveguiding (cf. green  $k_{WG,lowloss}$ ) or essentially no losses due to total internal reflection at the crystal-substrate interface for very large angles. Hence, emission that propagates with angles larger than  $\theta_c$  into the substrate (or with in-plane wavevector components  $|k_i| > k_0$ ) is

waveguided within the 3TBT crystal (with small losses though as long as the criterion for total internal reflection at the crystal-substrate interface is not fulfilled), which corresponds to the criterion described in the manuscript text. In contrast, emission propagating under smaller angles than  $\theta_c$  into the substrate can leave the crystal at the top crystal-air interface and is quasi unguided (cf. gray wavevector  $k_{un}$ ). Note that the upper sketch in this figure is not to scale, because the in-plane wavevector component of a certain mode is constant across interfaces. The wavevectors are only meant to indicate the direction of propagation, not their magnitudes.

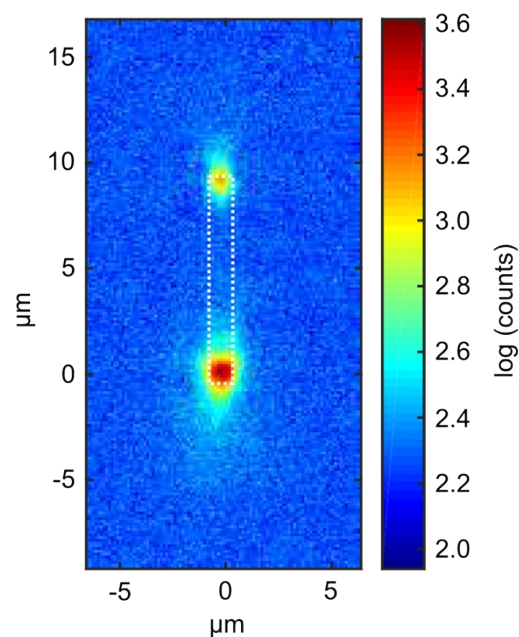


Figure S5: PL image of a 3TBT single crystal upon confocal excitation with a spot size of 500 nm at its bottom tip. The PL intensity is colour coded on a logarithmic scale. The PL from the top tip after waveguiding is clearly visible, whereas in between the tips no PL above the background signal is detectable, which indicates negligible loss of waveguided PL by scattering at surface defects. Note that this is the same crystal as that shown in Figure. 4d.

### Characteristic of the 3TBT single Crystal:

As reported recently<sup>1</sup>, the large 3TBT single crystals grown from solution at a relatively high crystallization temperature (60°C) exhibited needle-like morphology having a length of several hundred micrometers and a much smaller width of several micrometers. The

thickness, as measured by atomic force microscopy (AFM), of most crystals ranged from 2-7  $\mu\text{m}$ .

As expected for materials of high molecular order, 3TBT crystals were birefringent. Under crossed polarizers, these crystals exhibited a uniform intensity (birefringence) which varied when the crystals were rotated within the plane of observation<sup>1</sup>.

An AFM micrograph and the corresponding height profile of a 3TBT single crystal are shown in Figure S6.

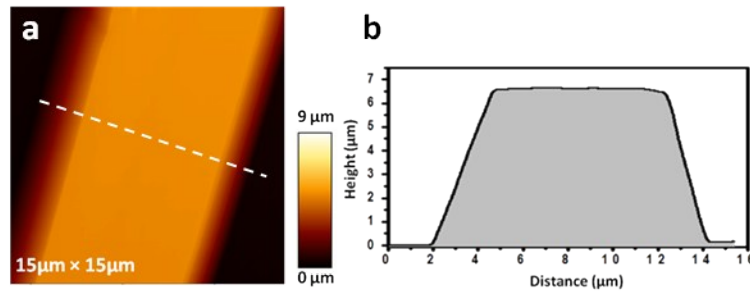


Figure S6. a) AFM height image of a 3TBT single crystal obtained by crystallization at 60 °C from a 0.1 g/L dodecane solution and spin-coated onto a solid substrate. b) Corresponding height profile along the white dashed line shown in a).

### Waveguide mode analysis:

We chose an approach put forward by Balzer et al.<sup>2</sup> to determine the refractive index and to show single- and multi-mode behaviour in our thin (300 nm) and thick (1  $\mu\text{m}$ ) crystals in Figure. 4 in the main manuscript: For waveguiding along a thin crystal, the spatially resolved spectra upon excitation at the crystal body (see Figure. 4c,f) feature a clear wavelength threshold (here, the threshold wavelength is  $\sim 600$  nm), whereas for the thick one there is no threshold in the observed PL wavelength range. Since the exact (anisotropic) refractive index of 3TBT crystals is unknown, we determine a range refractive indices based on the number of modes  $m$  for a given waveguided wavelength  $\lambda$  for a crystal with thickness  $a$

$$m < 2a/\lambda \sqrt{\frac{\epsilon_s}{\epsilon_p} \sqrt{\epsilon_p - \epsilon_3}} \quad (\text{see reference 2})$$

(dielectric constants  $\epsilon$ , with indices s: along the long axis of the crystal; p: perpendicular to crystal axis in plane of substrate (parallel to the transition dipole moment); 3: dielectric constant of glass substrate with  $\sqrt{\epsilon_3} = 1.5$ ).

The Figure S7 shows that a crystal with  $a < 300$  nm (and  $\lambda = 600$  nm) features single mode behaviour over a wide refractive index range between  $\sim 1.8$  and 2.3, which is in the range of the refractive index for crystalline thiophene based systems<sup>3</sup>. In contrast, for thicker crystals there is always multi-mode operation within the same refractive index range.

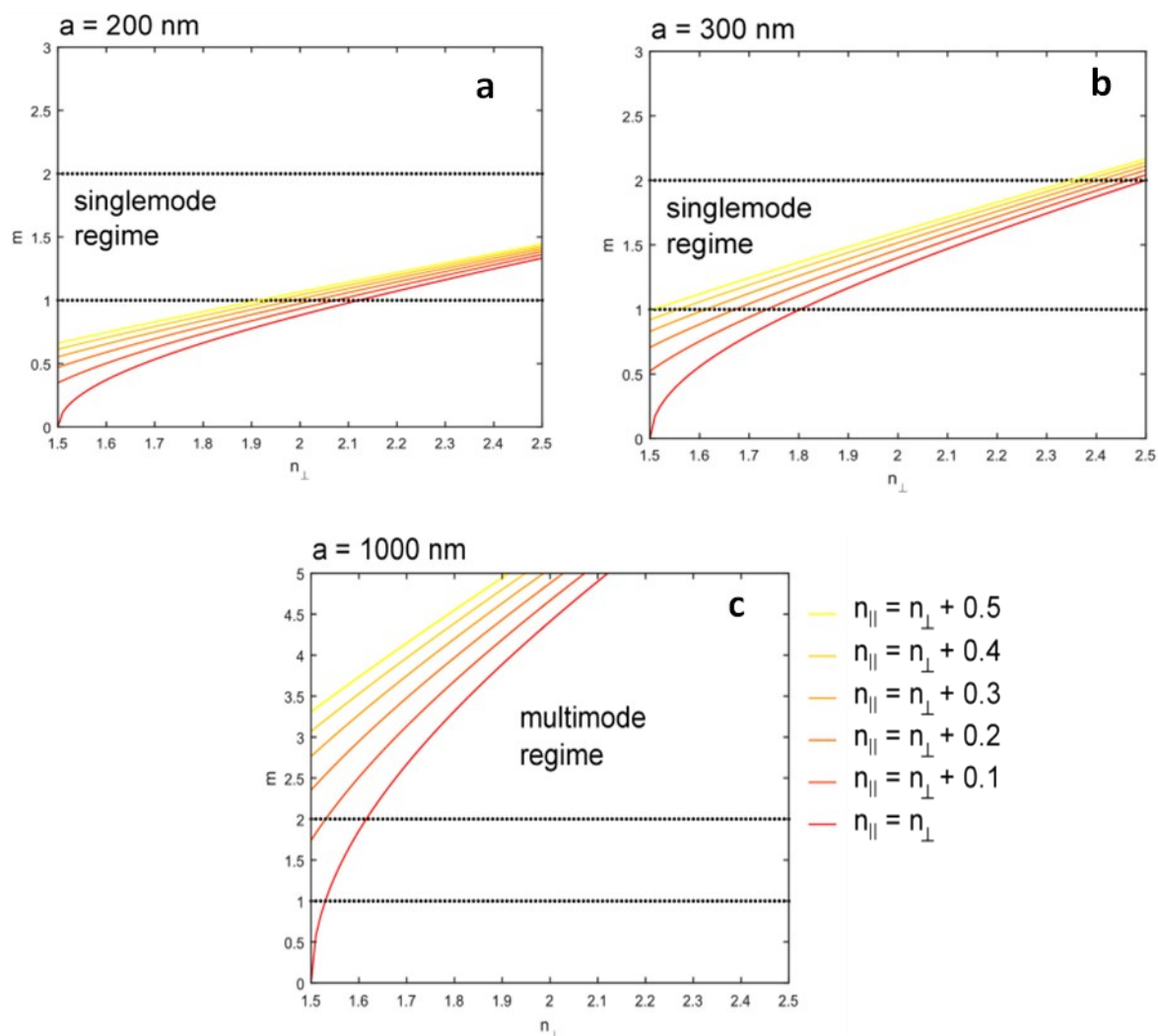


Figure S7. The number of waveguide modes  $m$  for a given waveguided wavelength  $\lambda = 600$  nm for a crystal with thickness a)  $a = 200$ . b)  $a = 300$  c)  $a = 1000$  nm.

## References:

- (1) Motamen, S.; Raithel, D.; Hildner, R.; Rahimi, K.; Jarrosson, T.; Serein-Spirau, F.; Simon, L.; Reiter, G. Revealing Order and Disorder in Films and Single Crystals of a Thiophene-Based Oligomer by Optical Spectroscopy. *ACS Photonics* **2016**, *3* (12), 2315–2323.
- (2) Balzer, F.; Bordo, V.; Simonsen, a.; Rubahn, H.-G. Optical Waveguiding in Individual Nanometer-Scale Organic Fibers. *Phys. Rev. B* **2003**, *67* (11), 115408.
- (3) Brown, P.; Thomas, D.; Köhler, A.; Wilson, J.; Kim, J.-S.; Ramsdale, C.; Siringhaus, H.; Friend, R. Effect of Interchain Interactions on the Absorption and Emission of poly(3-Hexylthiophene). *Phys. Rev. B* **2003**, *67* (6), 1–16.

